

Performance Improvement of Alternators With Switched-Mode Rectifiers

Juan Rivas, *Student Member, IEEE*, David Perreault, *Member, IEEE*, and Thomas Keim, *Member, IEEE*

Abstract—The use of a switched-mode rectifier (SMR) allows automotive alternators to operate at a load-matched condition at all operating speeds, overcoming the limitation of optimum performance at just one speed [1], [2]. While use of an SMR and load matching control enables large improvements in output power at cruising speed, no extra power is obtained at idle. This document introduces a new SMR modulation strategy capable of improving alternator output power at idle speed without violating thermal or current limits of the alternator. The new modulation scheme may be implemented with simple control hardware, and without the use of expensive current or position sensors. After introducing the new modulation method, we develop approximate analytical models that establish the underlying basis for the approach. Implementation considerations are addressed, and both simulation and experimental results are provided that demonstrate the advantages of the proposed control method.

Index Terms—Alternator, generator, idle, Lundell, rectifier, switched-mode rectifier (SMP).

I. INTRODUCTION

THERE HAS BEEN a continuous increase in electrical power demand in automobiles as a result of the electrification of existing loads and the introduction of new vehicle functions [3], [4]. One consequence of this increasing demand is that improvements in automotive generators are becoming necessary. As of today, Lundell-type alternators with diode rectifiers are almost universally used. The alternators are designed to operate optimally at idle speed, thus maximizing output power delivery at the speed providing the least generated power. At higher speeds, the power capabilities of the alternator machine are under-utilized. Recent work has demonstrated that introduction of a switched-mode rectifier (SMR) and appropriate control into the alternator can overcome this limitation [1], [2]. In this approach, the bottom diodes of the rectifier bridge are replaced by controlled switches [e.g., power metal-oxide semiconductor field-effect transistors (MOSFETs)] as shown in Fig. 1. This SMR allows matching of the effective voltage seen by the alternator to that required for maximum power at *any* speed. This operating mode, termed “load matching,” maximizes output power across the speed range. An experimental comparison between conventional diode rectification and switched-mode rectification with load

matching is illustrated in Fig. 2. The practical implications of such a SMR with load matching control are clear: the average output power capability of the alternator over normal driving cycles is increased. Additional advantages of this approach are described in [1] and [2].

A major limitation of the load-matched control technique is that even though the alternator works optimally at any speed, it does not improve alternator performance at idle speed (Fig. 2). Some present and future installed functions in cars will require higher electrical power at cruising speed (e.g., electromagnetic valves, water pumps, etc.) making the SMR a good solution for dealing with that demand. On the other hand, many other applications will benefit from power improvements at all speeds, including idle. Thus, the described approach is still limited by the already-optimized-at-idle alternator. Design and control approaches which can improve output power at idle are therefore of particular value for future systems.

This paper introduces a new modulation technique for the SMR that achieves a significant increase in alternator output power at idle speed. The new modulation scheme may be implemented with simple control hardware, and without the use of expensive current or position sensors. After introducing the new modulation method, we develop approximate analytical models that establish the underlying basis for the approach. Implementation considerations are addressed, and both simulation and experimental results are provided that demonstrate the advantages of the proposed control method.

Section II of this paper describes the new modulation technique and develops the analytical models that underly it. Section IV of the paper addresses implementations of the proposed strategy including some of the design constraints and hardware issues, and describes the design of an experimental prototype system. Section V presents both simulation and experimental results from the implemented modulation technique that demonstrate the extra output power available at idle. Finally, Section VI draws conclusions and presents a preliminary evaluation of the approach.

II. SWITCHING MODULATION FOR IMPROVED PERFORMANCE AT IDLE SPEED

The existing load matching technique can be implemented on a three-switch boost rectifier (Fig. 1) by modulating the three switches of the SMR together at the same frequency and duty cycle, where the duty cycle is a function of speed (and possibly other variables). This paper presents a new modulation approach that takes the SMR control one step further by modulating the three SMR switches in Fig. 1 independently. This adds

Manuscript received July 10, 2003. Paper no. TEC-00171-2003. This work was supported by the member companies of the MIT/Industry Consortium on Advanced Automotive Electrical/Electronic Components and Systems. This paper was presented at the IEEE Power Electronic Specialist Conference in Acapulco, México, June 2003.

The authors are with the Massachusetts Institute of Technology, Cambridge, MA 02139 USA (e-mail: jmrivas@mit.edu).

Digital Object Identifier 10.1109/TEC.2004.832072

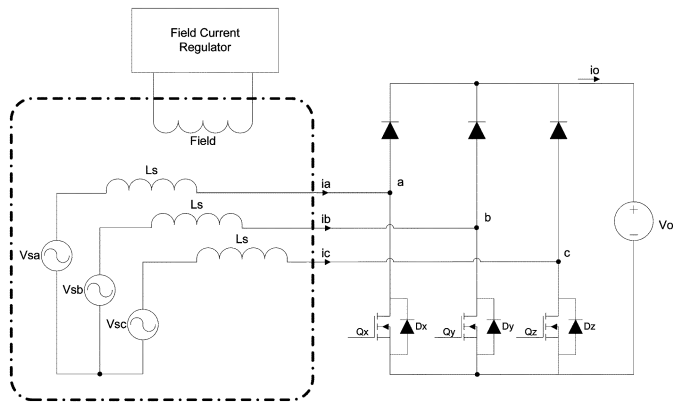


Fig. 1. Electrical model of a Lundell alternator connected to an SMR.

the necessary degrees of freedom to enable more power to be delivered at idle speed. Three important observations are worth mentioning about possible modulations using an SMR.

- The bottom MOSFETs of the SMR can only be effectively modulated while they carry positive current; during other periods, their corresponding back-diodes conduct.
- Any viable scheme must keep the alternator within allowed thermal limits.
- For the modulation scheme to be practical given automotive cost constraints, it should not require expensive sensors or controls.

In this paper, there will be a focus on techniques that do not incur other costs (e.g., requiring position or current sensors.)

It is expected that through the improved alternator performance that results from this work, the use of an SMR will be a better, yet economical, option for high-power alternators.

Fig. 3 shows the phase current and the instantaneous phase-to-ground rectifier voltage for one phase over an alternator electrical cycle. A simplified representation of one cycle of the SMR modulation technique developed here is shown on the same axes. The switching function for each of the legs of the structure is realized at a frequency many times higher than the line-current frequency and the duty cycle is modulated in such a way as to obtain the “local-average” phase-to-ground voltage v_{ag} shown in Fig. 3. Looking at this local average voltage waveform it is possible to define the different intervals that describe the planned strategy under the new modulation scheme. The back EMF voltage v_{sa} is shown with a dotted line, while the current i_a is shown as a distorted sinusoid with a solid line. The pattern is the same for the other phases, but delayed by 120 electrical degrees of the fundamental.

The new modulation technique consists then of the following subintervals:

- δ : During this subinterval, beginning when the phase current becomes positive, the switch is kept on, forcing the phase-to-ground voltage to be near zero. During this δ portion, additional energy is stored in the winding inductance.
- Mid-cycle: Operation at a nominal duty ratio and average voltage V_{base} . This voltage is close to that for the load matching condition, and will be a function of the alternator speed.

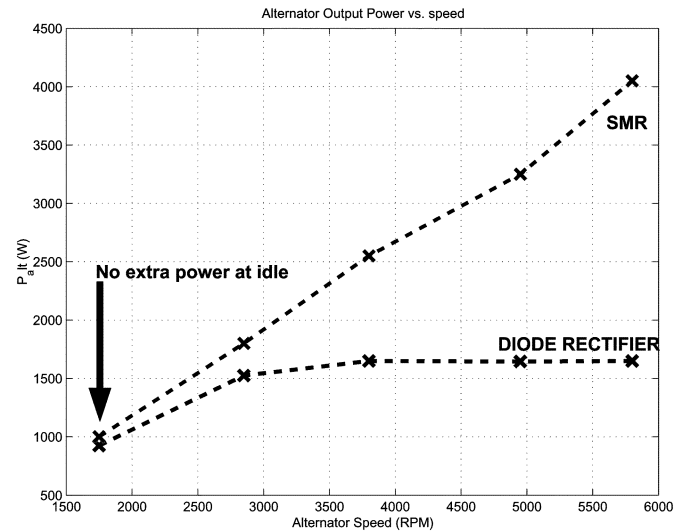


Fig. 2. Experimental comparison of the output power versus alternator speed using an SMR in load-matched operation and a regular diode bridge rectifier.

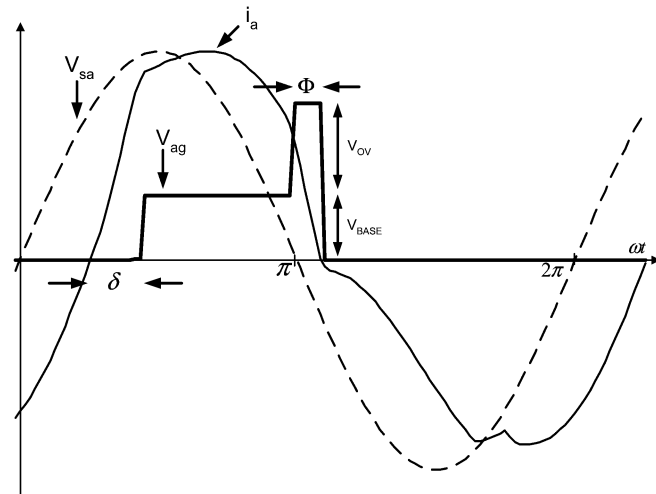


Fig. 3. Waveforms for new modulation technique.

- Φ : From the beginning of this interval to the end of the positive portion of the line current, the duty ratio is adjusted so as to obtain an average phase-to-ground voltage that exceeds the nominal V_{base} by V_{ov} volts.

The new modulation strategy embodied in Fig. 3 enables additional output power to be obtained from an alternator compared to that achievable with diode rectification or switched-mode-rectification with load matching control. At the same time, this new modulation is simple enough to be implemented with inexpensive control hardware and without the use of expensive current or position sensors. The zero crossing of the phase current waveform can be effectively detected by observing the phase-to-ground voltage during the field-effect transistor (FET) off state. We have experimentally verified that this detection can be done simply and inexpensively. Achieving improved performance without significant increase in cost is a central benefit of both the selected rectifier topology and of the new modulation strategy introduced here.

It should be noted that the structure of the SMR imposes limitations in the modulation strategy that result in asymmetric

stator current waveforms. This does not represent a problem in automotive alternators provided that the thermal limits of the alternator are not exceeded. The increase in alternator output power is—for many modulation conditions of interest—accompanied by an increase in power dissipation. The amount of extra power that can be obtained through the proposed modulation strategy is ultimately limited by the thermal capabilities of the electric machine. Thus, we adjust the modulation parameters to maximize output power, while staying within the temperature limits of the machine.

The power dissipation and the temperature in the alternator are both a function of the rotational speed. In particular, Fig. 4 shows some experimental measurements of the power dissipation and the temperature of an alternator running at 1800 r/min and near 3000 r/min. In [5] and [6], it is shown that a typical alternator reaches a maximum temperature when running at 3000 r/min. It can be seen in Fig. 4 that it is possible to increase the power dissipation at idle speed while not exceeding the normal temperature of operation of the alternator when running at 3000 r/min. This suggests that some degree of increased power dissipation at idle speed is permissible. In particular, the model of [5] and [6] suggests that at least a 15% increase in root mean square (rms) stator current at idle speed is allowable from a thermal standpoint in a typical alternator.

III. ANALYTICAL MODEL

By means of adding new degrees of freedom in the control of the SMR, it is possible to manipulate the state variables of the system beneficially. In particular, we adjust the magnitude and phase of the different harmonic components that constitute the phase currents to enhance the average power delivered to the output.

As mentioned in Section II, the new modulation introduces two new subintervals to the normal operation of the SMR. A conduction angle interval δ is introduced beginning when the phase current becomes positive, during which the bottom switch of the SMR is kept *ON*. In this subinterval, electrical energy is stored in the machine inductance (L_s) for release in another part of the conduction period. In the second new subinterval, a conduction angle interval Φ is introduced during which the duty cycle of the corresponding bottom switch is adjusted such that the local average of the voltage at the input of the SMR v_{ag} is set to a voltage V_{OV} volts higher than in the main interval. These two subintervals will produce a phase shift that reduces the total phase angle α between the back electromotive-force (EMF) voltage v_{sa} and the fundamental component of the phase current i_{a1} thus increasing the amount of real power obtained at idle speed (1800 r/min). Furthermore, these intervals can be used to increase the fundamental phase current, thereby increasing output power. The modulation strategy embodied by Fig. 3 achieves this within the modulation constraints of the semibrige SMR, and without requiring detailed position or current information.

Following an approach similar to that of [7] and [8], it is possible to analyze and characterize the behavior of the fundamental component of the phase currents in the presence of the proposed modulation scheme. The simplified circuit shown in

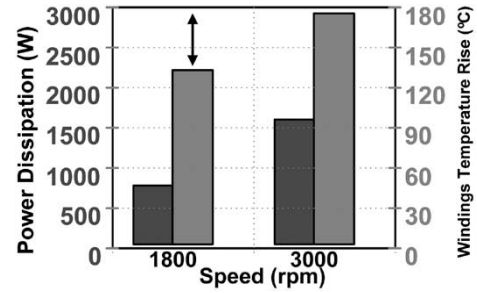


Fig. 4. Measured power dissipation and temperature of a Lundell alternator running at 1800 r/min and 3000 r/min.

Fig. 5 allows an intuitive and simple calculation of the current i_a for one phase. From that result, the output power delivered to the output voltage V_o and dissipation losses P_{diss} can be easily calculated by taking into consideration the contribution of the two other phase currents. It is also important to mention that in order to find a closed expression for the phase current, a symmetric conduction condition is assumed. Under this approximation, a positive current i_{a1} is assumed to circulate through the alternator's winding for exactly half of the current period (e.g., for $0 \leq \omega_o t \leq \pi$). The positive conduction angle of the current using the new modulation is not exactly 180° in practice, so that the symmetric conduction condition is not exact. Nevertheless, this approach provides a good insight into the operation and potential benefits of the proposed modulation scheme.

Looking at the circuit SMR structure shown in Fig. 1, we begin by defining the time-domain characteristic of the different back EMF voltage sources generated by the alternator. The magnitude V_{EMF} is given by $V_{EMF} = K_M \omega_s i_f$, where i_f is alternator field current, ω_s is alternator electrical frequency, and K_M is the machine constant in ($V \cdot s / \text{rad} \cdot A$). The back EMF voltages are

$$\begin{aligned} v_{sa} &= V_{EMF} \sin(\omega_s t) \\ v_{sb} &= V_{EMF} \sin\left(\omega_s t - \frac{2\pi}{3}\right) \\ v_{sc} &= V_{EMF} \sin\left(\omega_s t + \frac{2\pi}{3}\right). \end{aligned} \quad (1)$$

By applying *Kirchhoff's Voltage Law (KVL)* around the SMR structure for each of the phases, we can calculate the neutral-to-ground voltage v_{ng} which can be expressed as

$$\begin{aligned} v_{ng} &= -v_{sa} + Z_{RL} i_a + v_{ag} \\ v_{ng} &= -v_{sb} + Z_{RL} i_b + v_{bg} \\ v_{ng} &= -v_{sc} + Z_{RL} i_c + v_{cg}. \end{aligned} \quad (2)$$

Adding the three equations that describe the neutral-to-ground voltage v_{ng} , we obtain the following expression:

$$3v_{ng} = -\underbrace{(v_{sa} + v_{sb} + v_{sc})}_{=0} + Z_{RL} \underbrace{(i_a + i_b + i_c)}_{=0} + (v_{ag} + v_{bg} + v_{cg}). \quad (3)$$

As clearly shown in (3), the term $(v_{sa} + v_{sb} + v_{sc})$ is equal to zero, because the three back EMF voltage sources $v_{sa}(t)$, $v_{sb}(t)$, and $v_{sc}(t)$ form a three-phase set.

By applying the superposition principle, it can be seen that the phase-to-ground voltages at the three inputs of the SMR: $v_{ag}(t)$, $v_{bg}(t)$, and $v_{cg}(t)$ are

$$\begin{aligned} v_{ag} &= \langle v_{ag} \rangle + \widetilde{v}_{ag} \\ v_{bg} &= \langle v_{bg} \rangle + \widetilde{v}_{bg} \\ v_{cg} &= \langle v_{cg} \rangle + \widetilde{v}_{cg}. \end{aligned} \quad (4)$$

These voltage expressions are equal in magnitude, but phase shifted by $2\pi/3$ radians. This implies that the dc components for the three signals are the same $\langle v_{ag} \rangle = \langle v_{bg} \rangle = \langle v_{cg} \rangle$.

By plugging these expressions into (3) and solving for the neutral-to-ground voltage v_{ng} , we obtain

$$v_{ng} = \frac{1}{3} [\widetilde{v}_{ag} + \widetilde{v}_{bg} + \widetilde{v}_{cg}] + \langle v_{ag} \rangle. \quad (5)$$

Equation (5) can be subtracted from the expression for the phase-to-ground voltage $v_{ag}(t)$ to obtain an equivalent voltage source v_{eqv} that can be used to analyze one phase of the system. Observe that v_{eqv} consists of a linear combination of the ac components of the phase-to-ground voltages of the different phases

$$v_{eqv} = v_{ag} - v_{ng} = \frac{2}{3}\widetilde{v}_{ag} - \frac{1}{3}\widetilde{v}_{bg} - \frac{1}{3}\widetilde{v}_{cg}. \quad (6)$$

In order to obtain an equation for the phase current i_a from the circuit presented in Fig. 5, it is necessary to obtain the ac components of the voltages at the input of the SMR: \widetilde{v}_{ag} , \widetilde{v}_{bg} , and \widetilde{v}_{cg} so that an analytical description of the equivalent voltage source v_{eqv} can be obtained.

We can describe the voltage v_{ag} in terms of its Fourier series description

$$v_{ag} = a_0 + \sum_{n=1}^{\infty} a_n \cos(n\omega_0 t) + \sum_{n=1}^{\infty} b_n \sin(n\omega_0 t). \quad (7)$$

The fundamental component of the phase current i_{a1} is the only frequency component of the Fourier series representation of the current waveform i_a that actually contributes to real output power. By shifting all of the signals shown to the left, such that the reference angle is at the end of the interval δ , we can find a simple expression for the coefficients a_1 and b_1 of the Fourier series representation

$$a_1 = \frac{V_{base} + V_{ov}}{\pi} \sin(\delta) - \frac{V_{ov}}{\pi} \sin(\delta + \Phi) \quad (8)$$

$$b_1 = \frac{V_{base}}{\pi} + \frac{V_{base} + V_{ov}}{\pi} \cos(\delta) - \frac{V_{ov}}{\pi} \cos(\delta + \Phi). \quad (9)$$

Fig. 6 shows the resultant equivalent circuit with which is possible to calculate the magnitude and phase of the fundamental component of the current i_{a1} . In this circuit, the phase angle between the fundamental component of the phase i_a and the back EMF voltage v_{sa} is called α . To simplify the analysis, Fig. 6 shows the phase equivalent voltage v_{eqv} magnitude expressed as $c_1 = \sqrt{a_1^2 + b_1^2}$ and its phase before the mentioned shift by δ as $\chi = \tan^{-1}(a_1/b_1)$. The machine impedance for one phase of the alternator can be expressed as $|Z_L| \angle \theta_Z = R_s + j(\omega L_s)$.

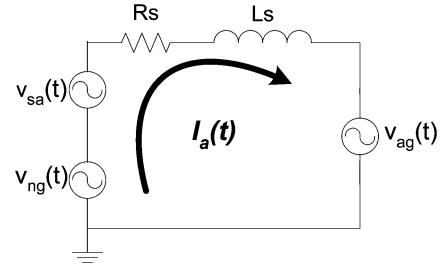


Fig. 5. Circuit model for one phase of the SMR.

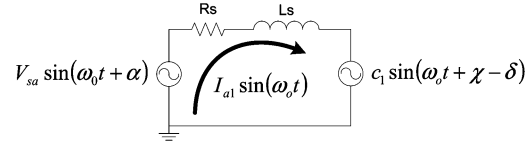


Fig. 6. Circuit model for the fundamental component of the waveforms of the SMR.

Solving the circuit shown in Fig. 6 by phasor analysis for the magnitude and phase of the fundamental component of the current i_{a1} , we obtain

$$|I_{a1}| \angle 0 = \frac{V_{sa}}{|Z_L|} \angle (\alpha - \theta_Z) - \frac{c_1}{|Z_L|} \angle (\chi - \delta - \theta_Z). \quad (10)$$

Expressing (10) in rectangular form, we obtain for real part (i.e., $\text{Re}\{i_{a1}\}$)

$$|I_{a1}| = \left[\frac{V_{sa}}{|Z_L|} \cos(\alpha - \theta_Z) - \frac{c_1}{|Z_L|} \cos(\chi - \delta - \theta_Z) \right]. \quad (11)$$

And for the imaginary part of (10) [i.e., $\text{Im}\{i_{a1}\}$]

$$0 = \left[\frac{V_{sa}}{|Z_L|} \sin(\alpha - \theta_Z) - \frac{c_1}{|Z_L|} \sin(\chi - \delta - \theta_Z) \right]. \quad (12)$$

Using (12), and solving for the phase difference α between v_{sa} and the fundamental of the phase current i_{a1} , we obtain

$$\alpha = \theta_Z + \sin^{-1} \left[\frac{c_1}{V_{sa}} \sin(\chi - \delta - \theta_Z) \right]. \quad (13)$$

Equation (13) can be substituted into (11) to solve for the magnitude of the fundamental component of the phase current, and it can be evaluated numerically. Using the aforementioned results and adding the contribution of the other two phases, it is possible to obtain a simple expression for the average output power $\langle P_{OUT} \rangle$

$$\langle P_{OUT} \rangle = 3 \left[V_{sa} I_{a1} \frac{\cos(\alpha)}{2} \right] - 3 \left[R_s \frac{I_{a1}^2}{2} \right]. \quad (14)$$

A. Model Validation

Using the results obtained in (11)–(14), we can simulate and plot the output power $\langle P_{OUT} \rangle$ and the approximate rms phase current versus one of the control parameters (e.g., δ), as illustrated in Fig. 7. The values that model the alternator parameters used for the simulation are related to the electrical model of the SMR presented in Fig. 1 and are $V_{saRMS} = 10.716$ V, $R_s = 37$ m Ω , $L_s = 120$ μ H, and $\text{freq} = 180$ Hz where V_{saRMS}

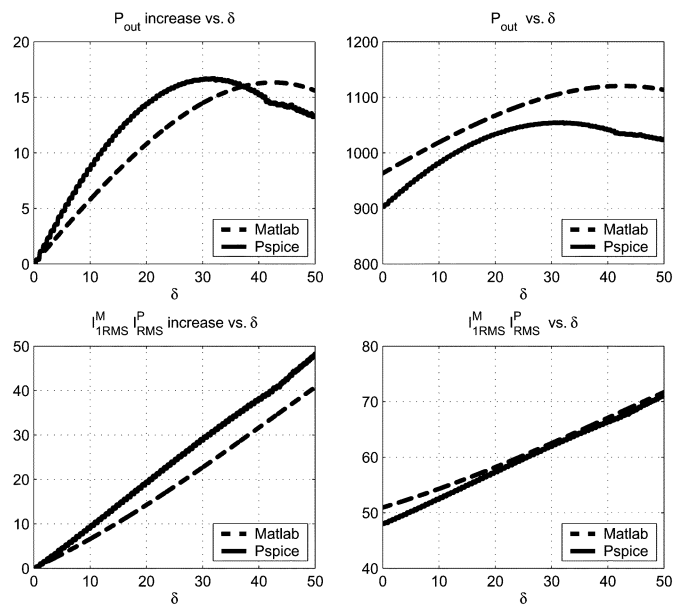


Fig. 7. Comparison between the MATLAB and PSPICE models versus the control parameter δ .

represents the back EMF at idle speed (e.g., electrical frequency $f_{\text{req}} = 180$ Hz) and full field current (e.g., $i_f = 3.6$ A), R_s is the winding resistance, and L_s is the machine inductance. The modulation parameters for the simulation shown in Fig. 7 correspond to $V_{\text{base}} = 14$ V, $V_{\text{OV}} = 0$ V the length of the interval is $\Phi = 0$. The δ parameter is varied from 0 to 50° . Fig. 7 also shows simulation results using a PSPICE model for the system described in the Appendix. There is close agreement between results obtained by the equation described in this paper and the circuit simulation using PSPICE. The principal differences between the results obtained are because the analytical model considered here only takes into account dissipation due to the fundamental component of the phase current, while the circuit simulation incorporates all dissipation components.

Simulation results show that a considerable amount of extra output power can be obtained by changing the length of the interval δ . They also show that the increase in real power is accompanied by a significant increase in phase current i_a . The increase in losses due to dissipation will set the limit for which this modulation will operate.

Fig. 8 shows the increase in output power $\langle P_{\text{OUT}} \rangle$ and the corresponding increase in rms phase current versus the parameter Φ . It can be seen that for small values of Φ , a small increase in phase current i_a is accompanied by a significant increase in output power. With bigger values of the control parameter Φ , it is possible to obtain a moderate increase in the output power but with an actual decrease in the magnitude of the phase current. This implies that is possible to obtain an increased amount of output power with lower loss. The difference that exists between the simulation and the numerical predictions arise because interval Φ is not small any longer; thus, the symmetric conduction condition is not achieved.

In order to explore how the output power depends on the control parameters δ and Φ , a PSPICE simulation model was used to realize a full grid search over those parameters. The output power increase and the phase current increase predicted by the

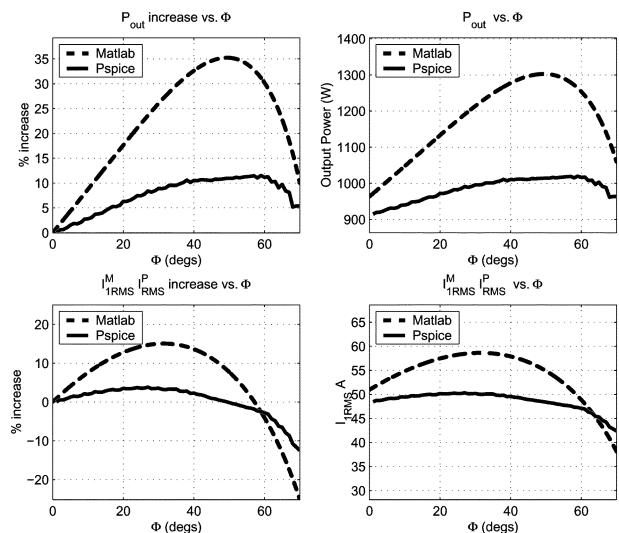


Fig. 8. Comparison between the MATLAB and PSPICE models versus the control parameter Φ .

simulation over the control range are presented in Figs. 9 and 10. As mentioned before, the amount of extra output power that can be obtained using the new technique presented in this paper is limited by the maximum allowable increase in conduction losses in the alternator windings. Fig. 9 also highlights the loci of the maximum obtainable increase in output power, when the increase in rms phase current is limited to 15%. This limit was selected in order to keep the alternator within acceptable thermal limits.

Fig. 11 shows the projections of the locus shown in Fig. 9 onto the three planes bounding the figure. This illustrates the output power increase that can be obtained by adjusting the parameters as indicated in the projection on the floor of the graph. The simulations predict that a 22% increase in output power can be obtained at idle while keeping the alternator within thermal limits.

IV. PROTOTYPE SYSTEM DESIGN

A prototype system (Fig. 12) has been developed to demonstrate the proposed modulation technique. This setup consists of an alternator that is driven with a three-phase motor, an SMR of the type illustrated in Fig. 1, and a controller. An electronic load (not shown) simulates the battery connected to the SMR system.

Accurate timing of the modulation with respect to the alternator phase currents is of great importance in realizing the proposed modulation scheme. This can be achieved using sensors to acquire information about the line currents from which the different subintervals are determined. The proposed modulation scheme only relies in very basic information about the sign of the phase currents. In the prototype system, this information is obtained through the use of Hall-effect current sensors and an incremental position encoder, though these would not be necessary in practice. Separately, we have experimentally demonstrated that the desired timing information can be obtained with only phase-to-ground voltage sensors. In our current prototype, the different parts of the modulation

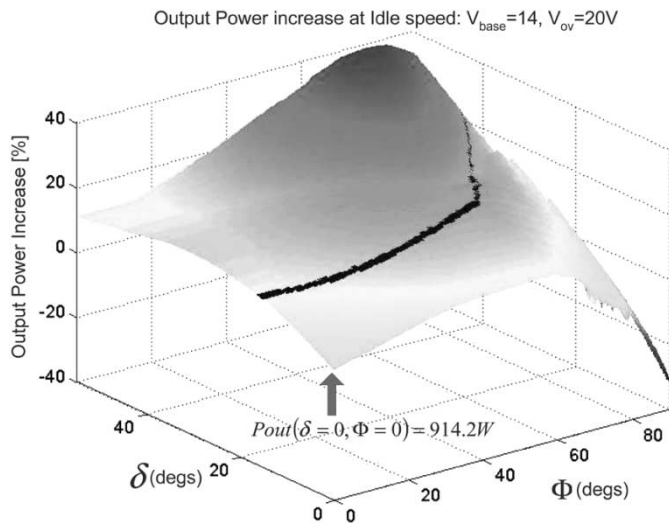


Fig. 9. Output power increase (%) versus δ and Φ for $V_{ov} = 20$, $V_{base} = 14$. Also shown is the locus on which the rms phase current is 15% higher than regular operating conditions.

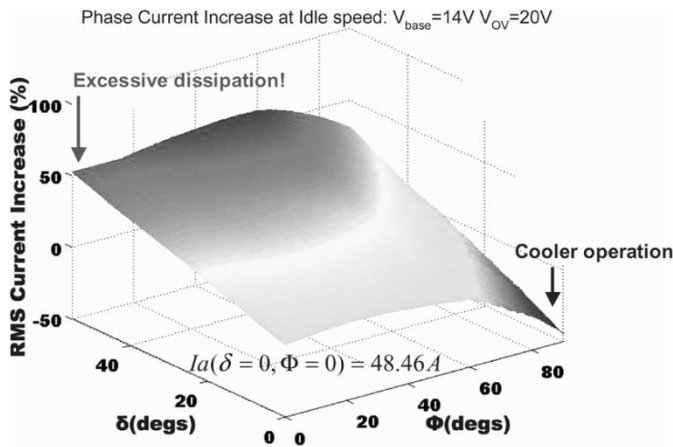


Fig. 10. RMS phase current increase (%) versus δ and Φ for $V_{ov} = 20$, $V_{base} = 14$.

switching control signals are generated using a small FPGA *XS40005XL*. It may be expected that the proposed modulation scheme will result in little incremental cost over a system with an SMR and load-matching control. Fig. 13 illustrates the duty-cycle variations of the MOSFET gating signals in relation to the corresponding phase currents. In the actual system, the switches are modulated at 100 kHz, much higher than the alternator electrical frequency (~ 180 Hz).

V. EXPERIMENTAL RESULTS

This section presents some experimental results obtained using the prototype system described in Section IV. We first validate the PSPICE averaged models used to search for preferred operating points. Fig. 14 shows the measured phase current i_a for the operating condition $\delta = 11.3^\circ$ and $\Phi = 0^\circ$ with $i_f = 3.6$ A, $V_{base} = 14$ V, $V_{OV} = 0$ V, and freq = 180 Hz. The same figure also shows the current waveform simulated using PSPICE for the same conditions. Close agreement between the average models and the experimental measurements is observed. Fig. 15 shows another operating condition ($\delta = 15^\circ$,

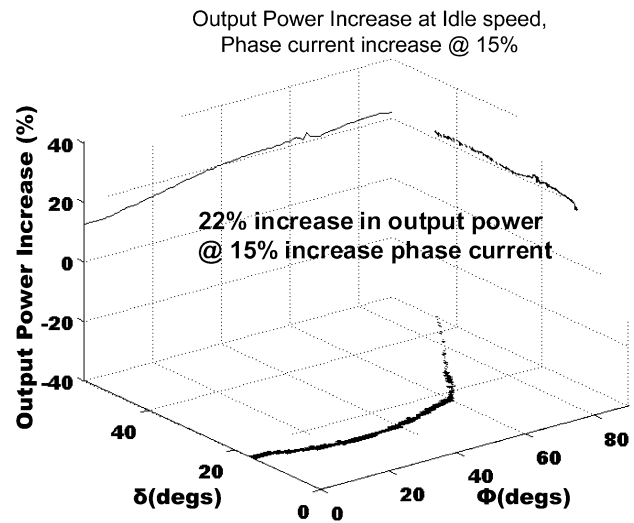


Fig. 11. Output power increase (%) versus δ and Φ for $V_{ov} = 20$, $V_{base} = 14$ when phase current increase is limited to 15%.

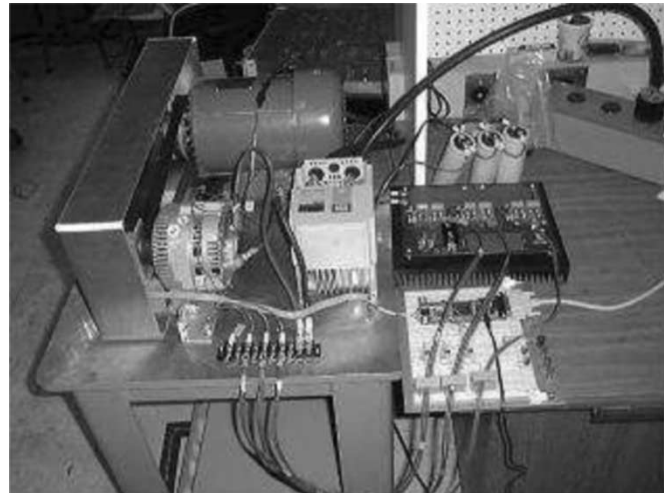


Fig. 12. Prototype setup.

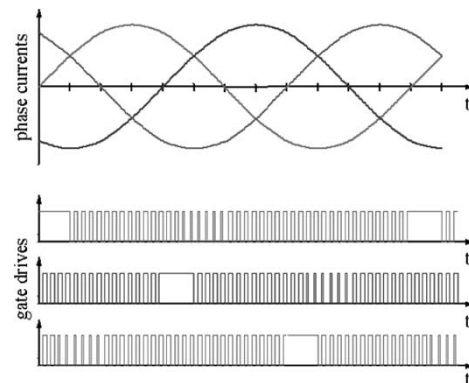


Fig. 13. Illustration of the modulation patterns of the SMR switches in relation to the phase currents.

$\Phi = 53.8^\circ$ and $V_{OV} = 18.7$ V $i_f = 3.6$ A, $V_{base} = 14$ V, and freq = 180 Hz at idle speed). Again, excellent agreement between simulation and experiment is observed. Fig. 16 shows experimentally measured increases in output power and the corresponding increases in phase current for a variety of

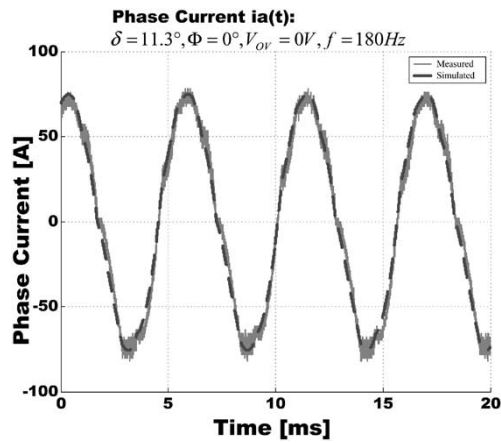


Fig. 14. Experimental and simulated phase current i_a at idle speed and maximum field current. $\delta = 11.3^\circ$, $\Phi = 0^\circ$, $V_{OV} = 0V$, $V_{base} = 14V$.

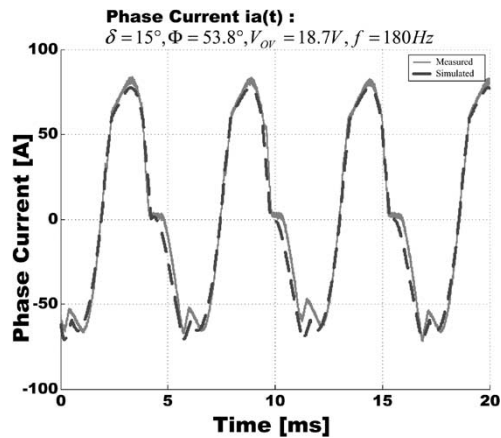


Fig. 15. Experimental and simulated phase current i_a at idle speed and maximum field current. $\delta = 15^\circ$, $\Phi = 53.8^\circ$, $V_{OV} = 18.7V$, and $V_{base} = 14V$.

operating conditions. These results show that for appropriate variations in Φ , significant increases in power delivery to the load can be achieved in combination with a reduction in the rms phase currents and associated losses. Furthermore, it is clear from these results that a significant increase in output power ($\sim 15\%$ or more) is achievable with limited (and acceptable) increases in rms phase currents and losses.

VI. CONCLUSION

While use of an SMR and load matching control alone enable big improvements in output power at cruising speed, no extra power is obtained at idle. This document introduced a new SMR modulation strategy capable of improving alternator output power at idle speed without violating thermal or current limits of the alternator. After introducing the new modulation method, approximate analytical models were developed that demonstrated the feasibility of this new approach. Implementation considerations were addressed, and both simulation and experimental results demonstrating the approach were presented. It may be concluded from these results that use of an SMR and the new modulation strategy provides a valuable increase in output power at idle speed. The technical feasibility

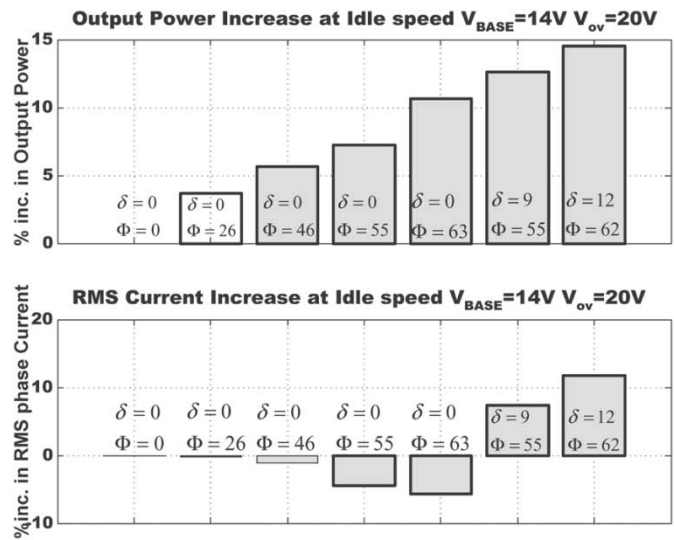


Fig. 16. Measure increase in output power and rms phase current at idle speed.

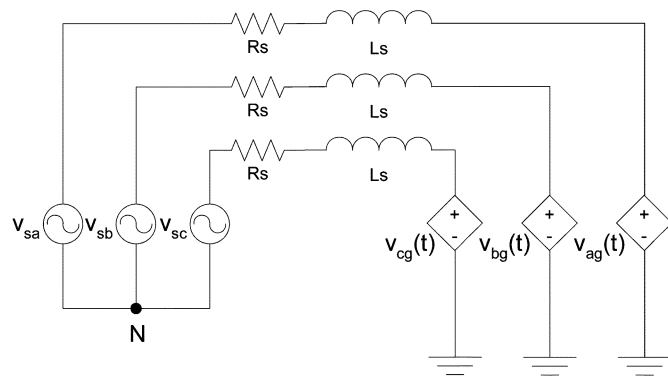


Fig. 17. PSPICE circuit model for the SMR power enhancement modulation.

of this new method has been demonstrated analytically—in simulation and experimentally. Achieving improved performance without significant increase in cost is a central benefit of both the selected rectifier topology and of the new modulation strategy introduced in this document.

APPENDIX PSPICE MODEL

An averaged PSPICE model was developed to validate the analytical model and to explore the parameter space (to optimize performance of the SMR). In order to reduce the time of the calculations required, the simulation makes use of averaged models instead of high-frequency switching models. Fig. 17 shows the structure of the PSPICE averaged model. In particular, it shows the alternator parameters V_{sx} (the back EMF voltage of the x phase), R_s , and L_s (the alternator’s winding resistance and inductance). The modulation technique presented in this paper was implemented using dependent voltage sources connected to each phase of the alternator. In particular, v_{ag} , v_{bg} , and v_{cg} each generate the corresponding neutral-to-ground voltage as determined by the new modulation shown in Fig. 3. The output power P_{OUT} and the I_{RMS} phase current were obtained by an analog circuit implemented in the simulation to ensure fast acquisition of the results.

The different parameters of the simulation δ , Φ , V_{OV} , and V_{base} can be independently controlled and varied thus making this a flexible simulation tool for this new power-enhancing technique. Details about the PSPICE model may be found in [9].

ACKNOWLEDGMENT

The authors would like to thank Prof. J. Kassakian of MIT for his input and support. The authors also thank W. Ryan of MIT for his help with the experimental realization of the new technology.

REFERENCES

- [1] D. J. Perreault and V. Caliskan, "Automotive Power Generation and Control," Massachusetts Institute of Technology, Cambridge, MA, Tech. Rep. TR-00-003, LEES, 2000.
- [2] —, "A new design for automotive alternators," in *Proc. IEEE/SAE Int. Congr. Transportation Electronics (Convergence)*, 2000, SAE paper 2000-01-C084.
- [3] J. M. Miller, D. Goel, D. Kaminski, H. P. Shöner, and T. M. Jahns, "Making the case for a next generation automotive electrical system," in *Proc. IEEE/SAE Int. Conf. Transportation Electronics (Convergence)*, Oct. 1998, SAE paper 98C-0006, pp. 41–51.
- [4] J. G. Kassakian, "Automotive electrical systems- the power electronics market of the future," in *Proc. IEEE Applied Power Electronics Conf. Expo.*, vol. 1, New Orleans, LA, Feb. 2000, pp. 3–9.
- [5] S. C. Tang, T. A. Keim, and D. J. Perreault, "Thermal modeling of Lundell alternators," *IEEE Trans. Energy Conversion*, submitted for publication.
- [6] —, "Thermal Analysis of Lundell Alternator," MIT/Industry Consortium on Advanced Automotive Electrical/Electronic Components and Systems, MIT Consortium Project Rep., 2002.
- [7] V. Caliskan, D. J. Perreault, T. M. Jahns, and J. G. Kassakian, "Analysis of three-phase rectifiers with constant-voltage loads," in *Proc. Power Electronics Specialists Conf.*, vol. 2, 1999, PESC 99, pp. 715–720.
- [8] —, "Analysis of three-phase rectifiers with constant-voltage loads," *IEEE Trans. Circuits Syst. I*, vol. 50, pp. 1220–1225, Sept. 2003.
- [9] J. M. Rivas, "Output Power Increase at Idle Speed in Alternators," Master's, Dept. Electrical Engineering and Computer Science, Massachusetts Institute of Technology, Cambridge, MA, 2003.



Juan Rivas (S'01) was born in México City, México. He received the B.A.Sc. degree in electrical engineering from the Monterrey Institute of Technology, México City, in 1998, and the S.M. degree from the Massachusetts Institute of Technology (MIT), Cambridge, in 2003. He is currently pursuing the Ph.D. degree at MIT in the Laboratory for Electromagnetic and Electronic Systems.

From 1999 to 2000, he was with Coralesa, México City, designing emergency lighting systems. His research interests include power electronics, RF power converters, resonant converters, soft switching topologies, and control of power converters.



David Perreault (S'92–M'97) received the B.S. degree from Boston University, Boston, MA, in 1989, and the S.M. and Ph.D. degrees from the Massachusetts Institute of Technology (MIT), Cambridge, in 1991 and 1997, respectively.

Currently, he is the Carl Richard Soderberg Associate Professor of Power Engineering with the MIT Department of Electrical Engineering and Computer Science. In 1997, he joined the MIT Laboratory for Electromagnetic and Electronic Systems as a Post-doctoral Associate, and became a Research Scientist in the laboratory in 1999. His research interests include design, manufacturing, and control techniques for power-electronic systems and components, in their use in a wide range of applications.

Dr. Perreault received the Richard M. Bass Outstanding Young Power Electronics Engineer Award from the IEEE Power Electronics Society and an ONR Young Investigator Award, and is a member of Tau Beta Pi and Sigma Xi.



Thomas Keim (M'90) received the B.S.M.E. degree from Carnegie-Mellon University, Pittsburgh, PA, and the S.M.M.E. and Sc.D. degrees from the Massachusetts Institute of Technology, Cambridge.

His professional experience includes work in General Electric Corporate Research and Development Center and Kaman Electromagnetics Corp., Hudson, MA. Since 1998, he has been Director of the MIT/Industry Consortium on Advanced Automotive Electrical/Electronic Components and Systems. He has 34 publications and nine patents, and is currently active both as an author and an inventor.